THE PENNSYLVANIA STATE UNIVERSITY
SCHREYER HONORS COLLEGE

DEPARTMENT OF PHYSICS

# Cross Sections of High-Energy Neutrinos

HENRY LI
SPRING 2024

A thesis
submitted in partial fulfillment
of the requirements
for baccalaureate degrees
in Physics and Mathematics
with honors in Physics

Reviewed and approved* by the following:

Anna Staśto
Professor of Physics
Thesis Supervisor

Sarah Shandera
Associate Professor of Physics
Honors Adviser

* Electronic approvals are on file in the Schreyer Honors College.

# Abstract

We study the cross sections for the collisions between high-energy neutrinos and nucleons. We compute the power of the energy behavior of the cross section for the neutral and charged current cases and find that in the limit of high energies it is approximately equal to 0.3, thus reflecting the behavior of the quark distributions as a function of small Bjorken $x$. We compute the ratios of the charm contribution to the total cross section. We implement the Monte Carlo method for the integration of the cross section. Finally, we study the inelasticity distribution and the average inelasticity as a function of neutrino energy in the cross section with the heavy quarks.

# Table of Contents

# List of Figures

# List of Tables

# Acknowledgements

I would like to express my gratitude to Dr. Anna Staśto for her advising me during my honors project. Her guidance and support have helped me understand research topics that were not covered in my undergraduate curriculum. With her generous help, I gained much understanding of my research topic and completed my honors project. It has been a wonderful experience working under Dr. Staśto's guidance. I would also like to express my gratitude to Honors Adviser Dr. Sarah Shandera.

# Chapter 1

# Introduction

## 1.1 Interactions Between Neutrinos and Other Particles

Neutrinos are electrically neutral elementary particles with extremely low masses. Currently, three types of neutrinos are known: the electron neutrino ($\nu_e$), muon neutrino ($\nu_\mu$), and tau neutrino ($\nu_\tau$). In addition, there are three types of antineutrinos, each corresponding to one of the three aforementioned neutrinos [1]. Typically, neutrinos are produced after a particle decays. For example, in the fundamental decay of beta decay process, a neutron ($n$) decays into a proton ($p^+$), an electron ($e^-$), and an electron antineutrino ($\bar{\nu}_e$). The beta decay process can be written as follows [1].

$$n \to p^+ + e^- + \bar{\nu}_e \tag{1.1}$$

In addition to the beta decay process, neutrinos are produced in various other interactions [1]. For example, a neutrino can be produced when a pion $\pi$ decays into a muon $\mu$

$$\pi \to \mu + \nu \tag{1.2}$$

and when, in turn, a muon $\mu$ decays into an electron $e$

$$\mu^- \to e^- + \bar{\nu}_e + \nu_\mu \tag{1.3}$$

where in the final state there is one electron antineutrino and one muon neutrino. There is also similar reaction for $\mu^+$. Neutrinos interact with matter only via the weak interactions [2] (and of course gravitationally), so these particles are extremely difficult to detect. In fact, neutrinos often do not interact with other particles and pass through ordinary matter unimpeded [1]. For example, a neutrino with an energy of $E \sim 1$ TeV has an interaction length of

$$\mathcal{L}^\nu \sim 250 \times 10^9 \text{ g/cm}^3 \tag{1.4}$$

and therefore can travel long distances without being deflected or interacting with matter. Despite the fact that neutrinos hardly interact with matter, it is possible to detect neutrinos using specialized detectors [3]. For example, the IceCube Neutrino Observatory can detect high-energy neutrinos [2, 4]. Situated underneath Antarctic ice, the IceCube Neutrino Observatory detects particles which are created by the interaction between neutrinos and the ice. In this case, the neutrinos are not observed directly and are instead detected via electrically charged particles which are produced as a result of the neutrinos colliding with matter [5]. IceCube can measure neutrinos with energies greater than 10 GeV, and such neutrinos are classified as high energy neutrinos [6]. Such highly energetic neutrinos can be produced by extremely energetic cosmic events such as *pp* interactions between cosmic rays and gas in galaxy clusters, gamma ray bursts, and supernovae [2, 7, 8]. The detection and observation of ultrahigh energy neutrinos have a wide variety of applications. Since neutrinos can travel large astronomical distances, they can help probe extremely distant astronomical objects. Neutrinos can also be produced via interactions of cosmic rays in the atmosphere [9, 10]. Furthermore, these neutrinos can be used to study phenomena such as neutrino oscillations and interactions between neutrinos and ordinary matter [6, 11, 12, 13]. To better understand how neutrinos interact with matter and how neutrinos can be detected, it is crucial to study the cross section for neutrino-nucleon interactions. In this work, we shall focus on the neutrino-nucleon interactions at very high energies.

## 1.2 Kinematics of Neutrino Interactions

We shall focus on the neutrino-nucleon interactions which are the dominant ones in the limit of high energies. The interactions of neutrinos with electrons are subdominant at high energies, with exception of the Glashow resonance [14], which is the interaction of the electron antineutrino with electrons. As we shall see, the reason for this is the fact that the nucleon is composite object and the cross section is proportional to the distributions of quarks and gluons in the nucleon whose density increases at very high energies. A Feynman diagram of a deep inelastic neutrino-nucleon scattering is shown in Figure 1.1.

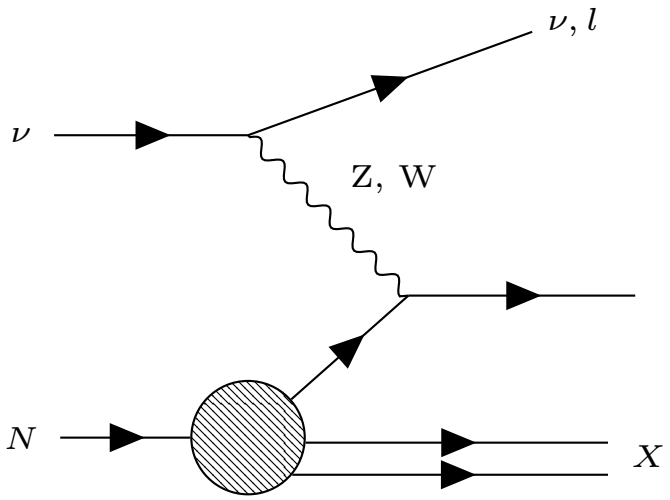


**Figure 1.1.** Diagram of deep inelastic neutrino-nucleon ($\nu$N) scattering. An intermediate Z or W boson is exchanged in a neutral current, and an intermediate W boson is exchanged in a charged current. X represents a system of hadrons.

During a deep inelastic neutrino-nucleon scattering, a vector boson (a neutrally charged Z boson or a charged W boson) is exchanged. The Z boson mediates a neutral current, and the W boson mediates a charged current.

Below we shall introduce the relevant variables for the deep inelastic neutrino nucleon scattering; for example, see [15].

We consider a system in which a neutrino ($\nu$) interacts with an nucleon ($N$); see Figure 1.1. In the lab frame, the neutrino moves with high energy towards the nucleon, which is at rest. The neutrino has a four-momentum of $p_\nu = (E_\nu, \vec{p_\nu})$ and the nucleon has a four-momentum of $p = (M, \vec{0})$. After the neutrino and the nucleon collide, a lepton (a neutrino or a charged lepton such as a muon) with four-momentum $k_l = (E_l, \vec{k_l})$ is produced [6]. To analyze the collision between the neutrino and the electron, we make use of various kinematic variables which are Lorentz invariants. Of particular interest are the center of mass energy $s$, the negative four-momentum transfer $Q^2 = -q^2$, and the inelasticity $y$. These three kinematic variables are defined as follows [16].

$$s = (p + p_\nu)^2 \tag{1.5}$$

$$-Q^2 = q^2 = (p_\nu - k_l)^2 \leq 0 \tag{1.6}$$

$$y = \frac{p \cdot q}{p \cdot p_\nu} \tag{1.7}$$

The inelasticity $y$ satisfies $0 \leq y \leq 1$ and represents the fraction of the neutrino's energy that is transferred to hadrons [17]. For $y = 0$, all of the neutrino's energy goes into the outgoing lepton. On the other hand, for $y = 1$, all of the neutrino's energy is carried away by the system of hadrons.

Furthermore, we define the Bjorken scaling variable $x$ using the following equation [16].

$$x = \frac{Q^2}{2p \cdot q} = \frac{Q^2}{2ME_\nu} \tag{1.8}$$

Neutrino-nucleon interactions (in the case of the incoming muon neutrino) may be expressed as

$$\nu_\mu N \to \mu^- + (anything), \tag{1.9}$$

in the charged current case and

$$\nu_\mu N \to \nu_\mu + (anything), \tag{1.10}$$

in the neutral current case. In practical applications one needs the cross section of neutrinos on nuclei. We shall not consider the nuclear effects in this work and for simplicity we shall consider the interaction on the isoscalar nucleon (i.e., a particle with equal numbers of protons and neutrons). We may treat $N$ as an average of a proton ($p$) and a neutron ($n$) [6]. In other words, we express N as follows [6]

$$N \equiv \frac{n+p}{2} \, . \tag{1.11}$$

## 1.3 Quarks

For the scattering of the neutrinos on the nucleon it is important to understand the nucleon structure. The nucleon is a composite object that consists of quarks and gluons, the latter being the mediators of the strong force. There are six quark flavors, which are also characterized by the different masses. The properties of quarks are given as follows.

**Table 1.1.** Quark Masses

| Quark Flavor | Mass (GeV/c$^2$) |
|---|---|
| Up (u) | 0.002 |
| Down (d) | 0.005 |
| Charm (c) | 1.3 |
| Strange (s) | 0.095 |
| Top (t) | 172 |
| Bottom (b) | 4.65 |

It is worth to note that since quarks are always confined, their masses are note well determined, especially for the lightest u,d,s quarks.

The nucleon is a composite particle that consists of quarks and gluons. Deep inelastic scattering experiments of electrons on protons allow for the measurement the distributions of quarks and gluons as a function of Bjorken $x$ variable and scale $Q^2$ [15]. These functions are called parton distribution functions, or PDFs and are usually denoted as

$$xq(x, Q^2), xg(x, Q^2). \tag{1.12}$$

The results of the DIS experiments, e.g. HERA [18], indicate that the quark and gluon distributions are increasing with the decreasing values of Bjorken $x$.

# Chapter 2

# Cross Sections of Neutrino-Nucleon Interactions

We would like to numerically obtain the contributions of different flavor quarks to the cross section. The procedure of numerically obtaining these contributions is outlined as follows. First, we numerically integrate the derivative of the cross section for each value of the neutrino energy. Then, we graph the cross section against the incoming neutrino energy. Finally, using the results of the cross section, we obtain the ratio of different quark flavors to the total and power dependence on the energy of the neutrino.

## 2.1 Cross Sections

The cross section $\sigma$ for a neutrino colliding with a nucleon is described by the following equation.

$$\sigma(E_\nu) = \iint dx\, dy \frac{d^2\sigma}{dx\, dy} \tag{2.1}$$

where $x$ is Bjorken variable and $y$ is the inelasticity.

The cross section in Equation 2.1 can be applied to both the neutral current which corresponds to the exchange of the $Z$ boson and the charged current which corresponds to the exchange of the $W$ boson. In a typical neutrino-nucleon collision, energy can be exchanged between the two particles through either current. The neutrino is incident upon the nucleon and causes quarks to be ejected from the nucleon. For a neutrino-nucleon collision, the term $\frac{d^2\sigma}{dx\, dy}$ can be computed in terms of the functions $xq$ and $x\bar{q}$. which correspond to the quark and anti-quark distributions in the nucleon.

### 2.1.1 Cross Section in Neutral Current

When a neutrino collides with a nucleon in the neutral current, one of four interactions the vector boson $Z$ can couple to the different quark flavors. This will lead to the production of the ($u\bar{u}$, $d\bar{d}$, $s\bar{s}$, $c\bar{c}$, $t\bar{t}$, and $b\bar{b}$) pairs. These six neutral current interactions contribute to the neutral current cross section.

In the neutral current (NC), we denote the cross section as

$$\sigma^{NC}(E_\nu) = \iint dx\, dy\, \frac{d^2\sigma^{NC}}{dx\, dy}. \tag{2.2}$$

In the neutral current, a neutrally-charged Z boson is exchanged between the neutrino and the nucleon. The cross section reads

$$\begin{aligned}\frac{d^2\sigma^{NC}}{dx\, dy} = {} & \frac{{G_F}^2 M E_\nu}{\pi}\left(\frac{{M_i}^2}{Q^2 + {M_i}^2}\right)^2 \\ & \cdot \left\{\frac{(1+(1-y)^2}{2}F_2^{NC}(x,Q^2) - \frac{y^2}{2}F_L^{NC}(x,Q^2) \pm y\left(1-\frac{y}{2}\right)xF_3^{NC}(x,Q^2)\right\},\end{aligned} \tag{2.3}$$

where $G_F$ is the Fermi constant, $M$ is the rest mass of the nucleon, and $M_Z$ is the mass of the Z boson. Functions $F_2^{NC}, F_L^{NC}, F_3^{NC}$ are the structure functions which parametrize the interaction between the neutrino and the nucleon in the neutral current case [6].

With Equations 2.2 and 2.3, we can numerically determine the cross section as a function of the energy. The cross section for the neutral current can be computed as follows.

$$\sigma^{NC}(E_\nu) = \iint dx\, dQ^2\, \frac{{G_F}^2 M E_\nu}{\pi} \left( \frac{{M_i}^2}{Q^2 + {M_i}^2} \right)^2 \cdot \left\{ \frac{(1+(1-y)^2}{2} F_2^{NC}(x,Q^2) - \frac{y^2}{2} F_L^{NC}(x,Q^2) \pm y \left(1 - \frac{y}{2}\right) x F_3^{NC}(x,Q^2) \right\}, \quad (2.4)$$

Therefore, we can numerically determine the cross section $\sigma^{NC}$ for each value of the energy $E_\nu$.

We see that the neutrino-nucleon cross section crucially depends on the behavior of the structure functions $F_i$. These in turn depend on the quark $xq(q, Q^2)$ and gluon distributions $xg(x, Q^2)$ in the nucleon. Thus, we need to have a model for the quark and gluon distributions which can be obtained from the QCD evolution. For the evaluations of the structure functions $F_i$ we used the calculation based on the small $x$ resummed evolution and the $k_T$ factorization. We used the results of the calculations and the code from [19].

We compute the values of the cross section by using numerical integration. The numerical calculations of the cross section as a function of energy of the neutrino are presented graphically in Figure 2.1, thus reproducing the results from [19].

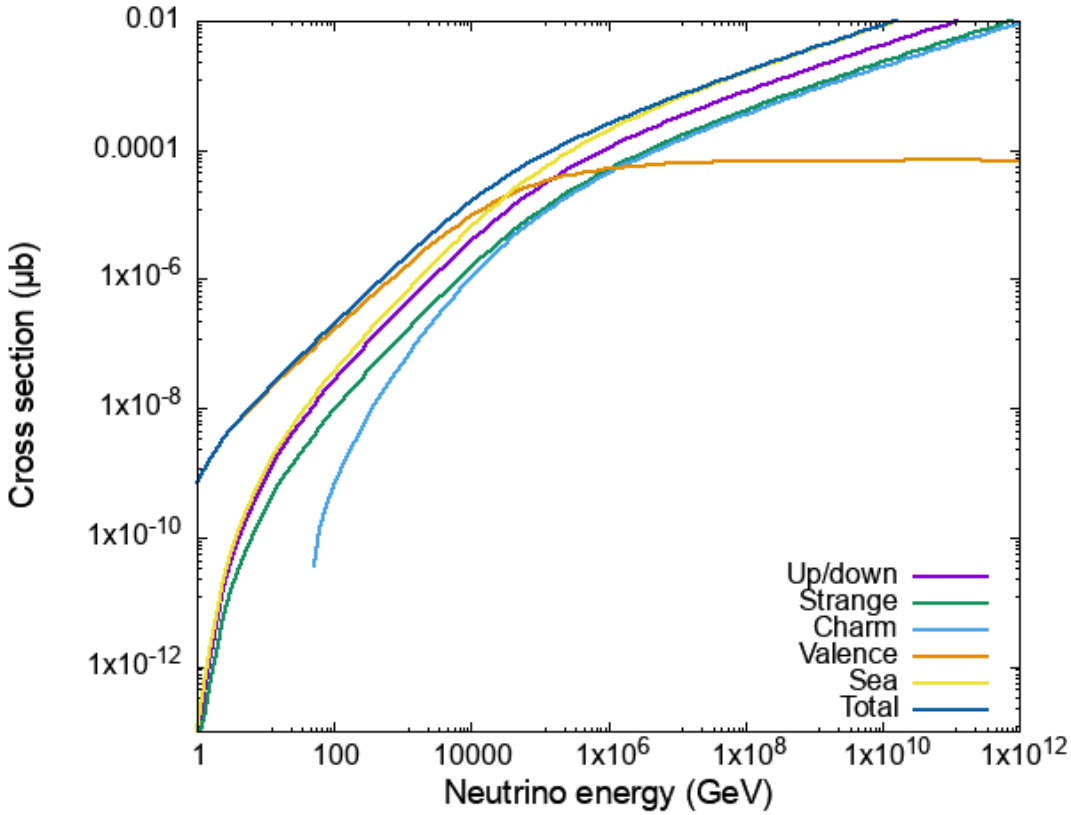


**Figure 2.1.** Neutrino-nucleon neutral current cross section as a function of neutrino energy.

As shown in Figure 2.1, the cross section increases with neutrino energy. Therefore, the more energetic a neutrino is, the greater the cross section of the neutrino; this trend holds for all flavors. In addition, Figure 2.1 shows that the rate of increase of the cross section with respect to the neutrino energy decreases as the energy increases.

### 2.1.2 Cross Section in Charged Current

When a neutrino collides with a nucleon in the charged current case, a quark and antiquark of different flavors are produced. There are three possibilities: $u\bar{d}$, $c\bar{s}$ and $t\bar{b}$ (and another three possibilities where the quark $\leftrightarrow$ antiquark). These three charged current interactions contribute to the charged current cross section. In the charged current (CC), we denote the cross section as

$$\sigma^{CC}(E_\nu) = \iint dx\, dy \frac{d^2\sigma^{CC}}{dx\, dy}. \tag{2.5}$$

In the charged current, an intermediate charged W boson is exchanged between the neutrino and the nucleon. The cross section for the charged current is

$$\begin{aligned}\frac{d^2\sigma^{CC}}{dx\, dy} &= \frac{{G_F}^2 M E_\nu}{\pi}\left(\frac{{M_i}^2}{Q^2 + {M_i}^2}\right)^2 \\ &\cdot \left\{\frac{(1+(1-y)^2}{2}F_2^{CC}(x,Q^2) - \frac{y^2}{2}F_L^{CC}(x,Q^2) \pm y\left(1-\frac{y}{2}\right)xF_3^{CC}(x,Q^2)\right\},\end{aligned} \tag{2.6}$$

where $M_W$ is the mass of the exchanged intermediate W boson. Using Equations 2.5 and 2.6, we obtain the following

$$\begin{aligned}\sigma^{CC}(E_\nu) &= \iint dx\, dQ^2\, \frac{{G_F}^2 M E_\nu}{\pi}\left(\frac{{M_i}^2}{Q^2 + {M_i}^2}\right)^2 \\ &\cdot \left\{\frac{(1+(1-y)^2}{2}F_2^{CC}(x,Q^2) - \frac{y^2}{2}F_L^{CC}(x,Q^2) \pm y\left(1-\frac{y}{2}\right)xF_3^{CC}(x,Q^2)\right\},\end{aligned} \tag{2.7}$$

Therefore, we can numerically compute the charged current cross section based on the energy of the incoming neutrino. The numerical results are presented graphically in Figure 2.2, again using the code from [19] and reproducing the results in that work.

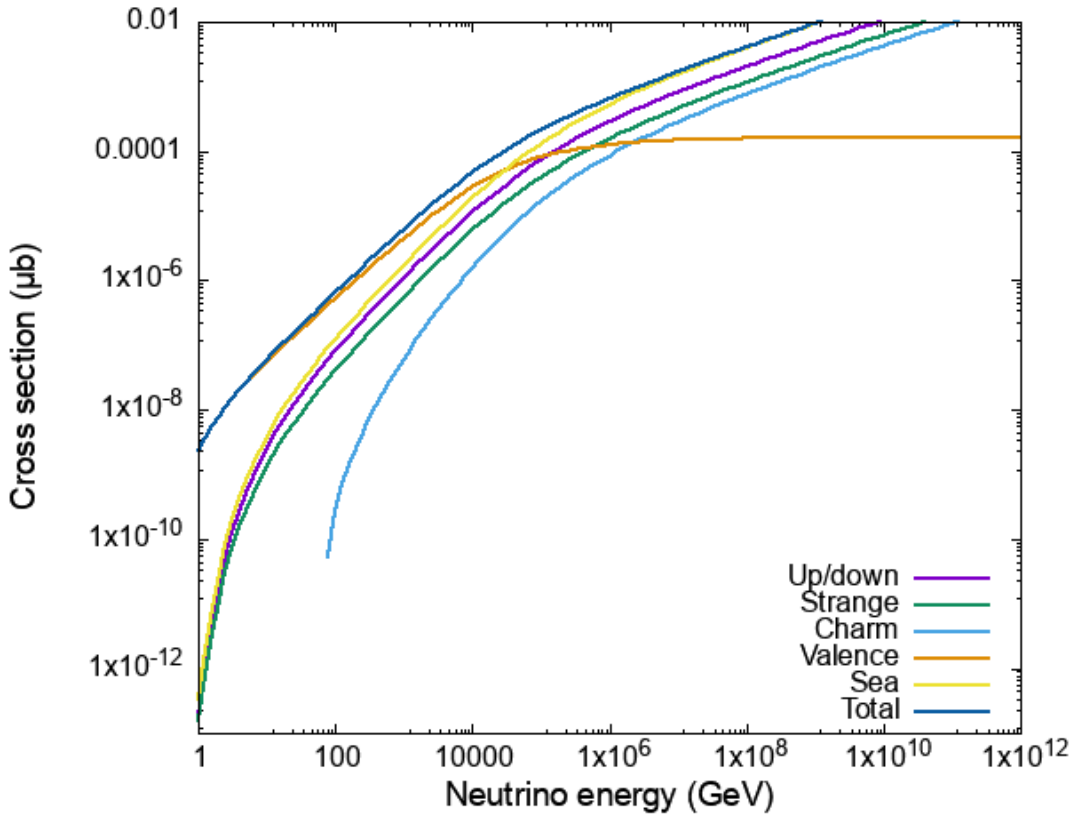


**Figure 2.2.** Neutrino-nucleon charged current cross section as a function of neutrino energy.

According to Figure 2.2, the cross section in the charged current increases as the neutrino energy increases. Therefore, the more energetic a neutrino is, the greater the cross section of the neutrino; this trend holds for all flavors. In addition, Figure 2.2 shows that the rate of increase of the cross section with respect to the neutrino energy decreases as the energy increases.

The cross section in the charged current is similar to that in the neutral current, since the neutral current and the charged current arise from similar mechanics (i.e., exchange of intermediate bosons and the similar dependence on the quark parton distributions). It is noteworthy that the cross section in the charged current is larger than that in the neutral current; the larger cross section in the charged current is due to the different prefactors stemming from the couplings (the chiral couplings in the case of the neutral current) [2].

## 2.2 Power Law Between Neutrino Energy and Cross Section

As shown in Figure 2.1 and Figure 2.2, the cross section increases with energy. However, the rate of the increase is different across different energy ranges. At first, the cross section increases faster, followed by a slower increase after the energy of about $10^5$ GeV. We shall

analyze the rate of increase by looking at the power governing the energy dependence of the cross section.

### 2.2.1 Power Law in Neutral Current

Based on the numerical calculations of the cross section and the neutrino energy, we determine a constant $\lambda$ in the high-energy regime such that

$$\sigma^{NC}(E_\nu) \sim {E_\nu}^{\lambda}. \tag{2.8}$$

In other words, we seek an appropriate exponent in the case of $E_\nu \to \infty$. From Equation 2.8, we obtain

$$\ln \sigma^{NC}(E_\nu) \sim \lambda \ln E_\nu. \tag{2.9}$$

By taking the derivative of Equation 2.9 with respect to $\ln E_\nu$, we get

$$\frac{d}{d(\ln E_\nu)}[\ln \sigma^{NC}(E_\nu)] \sim \lambda \tag{2.10}$$

Therefore, the above equation gives the numerical value of the exponent $\lambda$ for large values of $E_\nu$. The value of $\lambda$ can be numerically determined as follows.

$$\lambda = \lim_{E_\nu \to \infty} \frac{d[\ln \sigma^{NC}(E_\nu)]}{d(\ln E_\nu)} \tag{2.11}$$

Numerically, we must make an approximation for the derivative of $\ln \sigma^{NC}$. The approximation can be achieved by taking small incremental values of $\ln E_\nu$ and computing the increment of $\ln \sigma^{NC}$. The following approximation scheme is used.

$$\lambda = \frac{\ln \sigma^{NC}(E_{\nu,2}) - \ln \sigma^{NC}(E_{\nu,1})}{\ln E_{\nu,2} - \ln E_{\nu,1}}, \tag{2.12}$$

where $E_{\nu,1}$ and $E_{\nu,2}$ are different neutrino energy values. To implement the approximation, we use the following equation

$$\lambda = \frac{\ln \sigma^{NC}(E + \delta E) - \ln \sigma^{NC}(E)}{\delta E}, \tag{2.13}$$

where $E$ is an arbitrarily chosen neutrino energy value and $\delta E$ is an increment of the neutrino energy. Using Equation 2.13, we determine a function $\lambda$ with respect to $E$. The graph of $\lambda$ (exponent) versus $E_\nu$ (neutrino energy) is presented in Figure 2.3.

According to Figure 2.3, $\lambda$ decreases as $E_\nu$ of the incoming neutrino increases. For extremely high energies, the value of $\lambda$ approaches $\sim$0.3. Therefore, for the ultrahigh energy regime in the neutral current, the relationship between the cross section $\sigma$ and the energy of the neutrino $E_\nu$ is expressed as

$$\sigma^{NC}(E_\nu) \sim {E_\nu}^{0.3}. \tag{2.14}$$

The relationship between $\sigma^{NC}$ and $E_\nu$ given in the above relation is a key result, since it allows us to predict the approximate cross section of ultrahigh energy neutrinos based on the energy $E_\nu$ of the neutrinos.

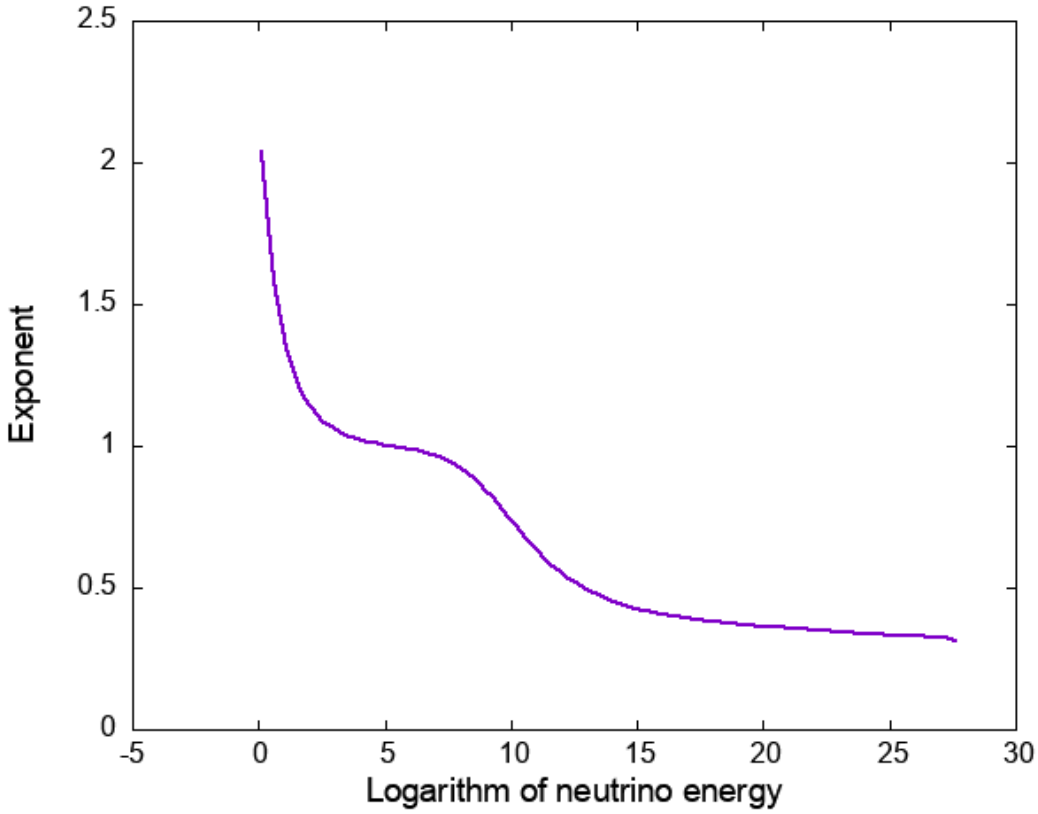


**Figure 2.3.** $\lambda$ (exponent) vs. $\ln(E_\nu/1\text{ GeV})$ for the neutral current cross section.

### 2.2.2 Power Law Charged Current

As in the neutral current, we can find a relationship between the cross section $\sigma^{CC}$ and the energy of an incoming neutrino $E_\nu$ in the charged current. By analogy to the equations presented in the preceding section, we postulate that $E_\nu$ and $\sigma^{CC}$ follow a relation

$$\sigma^{CC}(E_\nu) \sim {E_\nu}^{\lambda}. \tag{2.15}$$

We obtain the approximation scheme

$$\lambda = \frac{\ln \sigma^{CC}(E_{\nu,2}) - \ln \sigma^{CC}(E_{\nu,1})}{\ln E_{\nu,2} - \ln E_{\nu,1}}. \tag{2.16}$$

To implement the approximation, we use the equation

$$\lambda = \frac{\ln \sigma^{CC}(E + \delta E) - \ln \sigma^{CC}(E)}{\delta E}, \tag{2.17}$$

where $E$ is an arbitrarily chosen neutrino energy value and $\delta E$ is an increment of the neutrino energy. The graph of $\lambda$ (exponent) versus $E_\nu$ (neutrino energy) is presented in Figure 2.4.

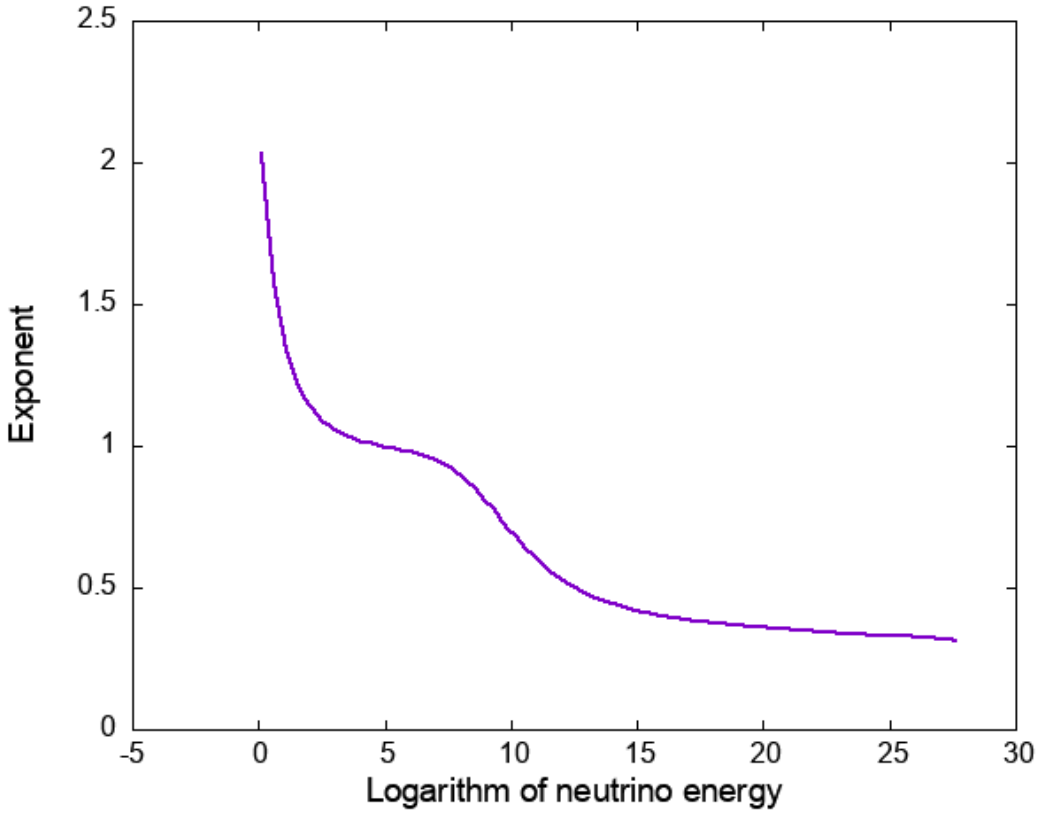


**Figure 2.4.** $\lambda$ (exponent) vs. $\ln(E_\nu/1\,\mathrm{GeV})$ for the charged current cross section.

According to Figure 2.4, $\lambda$ decreases as the neutrino energy $E_\nu$ increases. In the ultrahigh energy regime, $\lambda$ approaches a value of $\sim$0.3. Therefore, for extremely energetic neutrinos, we can predict the charged current cross section of the neutrino based on the energy of the neutrino. The relationship between $\sigma^{CC}$ and $E_\nu$ in the charged current is expressed as follows.

$$\sigma^{CC}(E_\nu) = {E_\nu}^{0.3} \tag{2.18}$$

The above relation has the same form as the one derived in the case of the neutral current. The similarity between the two equations indicates that, for extremely energetic neutrinos, the cross sections in neutral and charged currents have the same trend with respect to the neutrino energy.

The extracted power of the increase $\lambda \sim 0.3$ is entirely driven by the power of the parton distributions as a function of $x$. It is known [6, 19] that the parton distributions are very steeply increasing functions of the inverse of the Bjorken variable $x$

$$xq \sim x^{-\lambda}, \tag{2.19}$$

where indeed the power $\lambda$ is about 0.3 at small values of $x$. The growth of the quark distributions is driven by the QCD evolution. Therefore, the neutrino interactions at very high energy are very sensitive probes of the dynamics of partons at very small Bjorken $x$.

One can show, (e.g., [6], [19]) that the cross sections for neutrino-nucleon interactions is sensitive to the Bjorken $x$ values of approximately

$$x \simeq \frac{M_{W,Z}^2}{2ME_\nu} \, , \tag{2.20}$$

which for very high neutrino energies probes the very small values of Bjorken $x$ and thus is sensitive to the high density of quarks and gluons in the nucleon.

## 2.3 Ratios of Quark Contributions to the Total Contribution

We seek to analyze the ratios between the contributions to the cross sections. According to our analyses of the cross sections in Section 2.2, all quarks individually contribute to the cross sections ($\sigma^{NC}$ and $\sigma^{CC}$). In each of these quark contributions, the cross sections increase with respect to the neutrino energy ($E_\nu$). However, the ratios of the contributions are not uniform and vary for different values of the neutrino energy. For example, Figure 2.1 shows that the valence quark contribution is the dominant contribution for low energy values (i.e., $10^1$ to $10^5$ GeV) but becomes insignificant for high energy values (i.e., $> 10^5$ GeV). In both the neutral and charged currents, we will in particular focus on the ratios of the charm quark contribution to the total contribution. We also focus on the relationship between the sea and valence quark contributions to the total contribution in both neutral and charged current cross sections.

### 2.3.1 Ratios in Neutral Current

Using the calculated individual quarks contributions obtained in Section 2.2.1, we can obtain the ratios of the charm ($r_c$), valence ($r_v$), and sea ($r_s$) quark contributions to the total contribution. The charm contribution in the neutral current arises from a $c\bar{c}$ process.

We define $\sigma^c$, $\sigma^v$, $\sigma^s$ as the neutral current cross sections for the charm, sea, and valence quark contributions, respectively. Furthermore, we define $\sigma^{NC}$ as the total neutral current cross section. The ratios of the contributions can be easily computed as follows.

$$r_c = \frac{\sigma^c}{\sigma^{NC}} \tag{2.21}$$

$$r_s = \frac{\sigma^s}{\sigma^{NC}} \tag{2.22}$$

$$r_v = \frac{\sigma^v}{\sigma^{NC}} \tag{2.23}$$

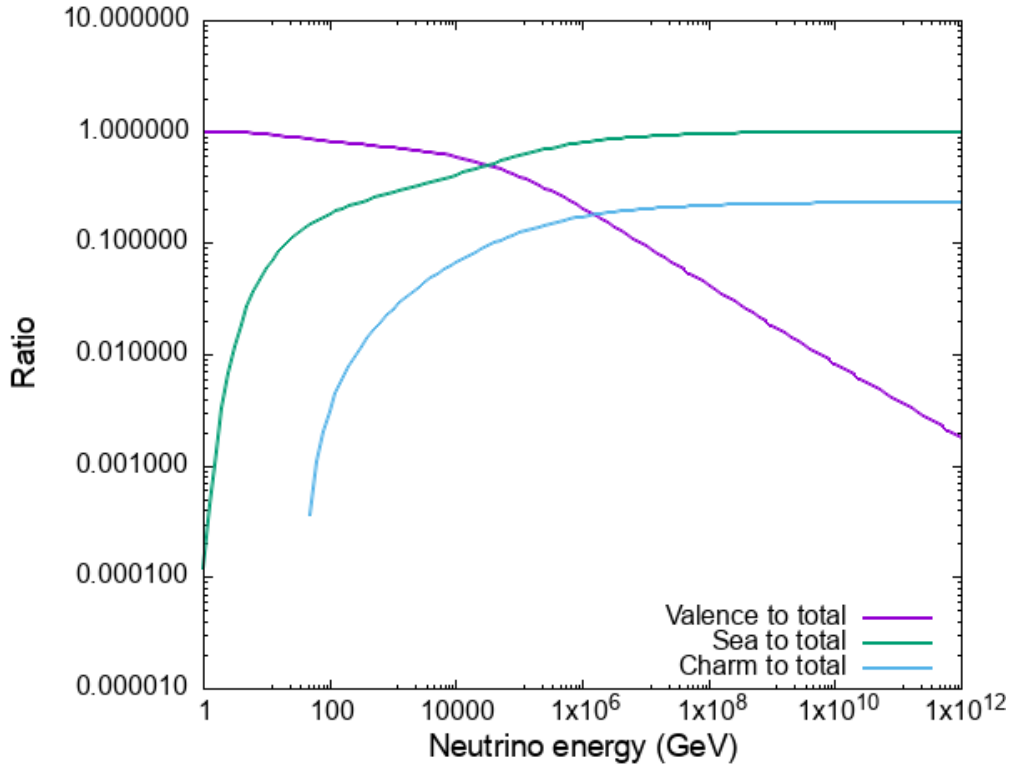


**Figure 2.5.** Ratios of different quark contributions to the total cross section in the neutral current case.

The ratios are functions of the neutrino energy $E_\nu$. We present the ratios graphically in Figure 2.5, which highlights the complementary relationship between the sea and valence quark contributions in the neutral current. The valence and sea quarks have different contributions depending on the neutrino energy. For low energy values, the valence quark contribution is much larger than the sea quark contribution and is therefore the dominant contribution. On the other hand, for high energy values, the sea quark contribution is instead the dominant contribution. In addition, Figure 2.5 shows how the charm contribution changes as the energy of the neutrino changes. Around a neutrino energy of $10^2$ GeV, the charm quark contribution is at a minimum. As the energy increases and is in the range of $10^4$ to $10^8$ GeV, the charm contribution increases. In other words, the more energetic a neutrino is, the greater the rate of charm production. However, for neutrino energy values greater than $10^8$ GeV, the increase in the charm contribution becomes less significant. As a result, a collision between extremely energetic neutrinos and nucleons does not produce appreciably more charm quarks compared to less energetic neutrino-nucleon collisions. The contribution of the charm quark to the total neutral current cross section is significant, about 20-25% at highest energies.

### 2.3.2 Ratios in Charged Current

We can similarly analyze the ratios of the charm, sea, and valence quark contributions in the charged current. One major difference between the neutral and charged currents is the

preservation of the flavor of quarks. Whereas the neutral current involves the exchange of an intermediate neutrally charged Z boson, the charged current involves the exchange of an intermediate charged W boson. As a result, the charm quark is transformed into a strange quark. We define $\sigma^{CC}$ as the total cross section in the charged current. By analogy to the definitions of the ratios of the neutral current, we define the ratios of the charm ($r_c$), valence ($r_v$), and sea ($r_s$) contributions in the charged current as follows

$$r_c = \frac{\sigma^c}{\sigma^{CC}} \tag{2.24}$$

$$r_s = \frac{\sigma^s}{\sigma^{CC}} \tag{2.25}$$

$$r_v = \frac{\sigma^v}{\sigma^{CC}} \tag{2.26}$$

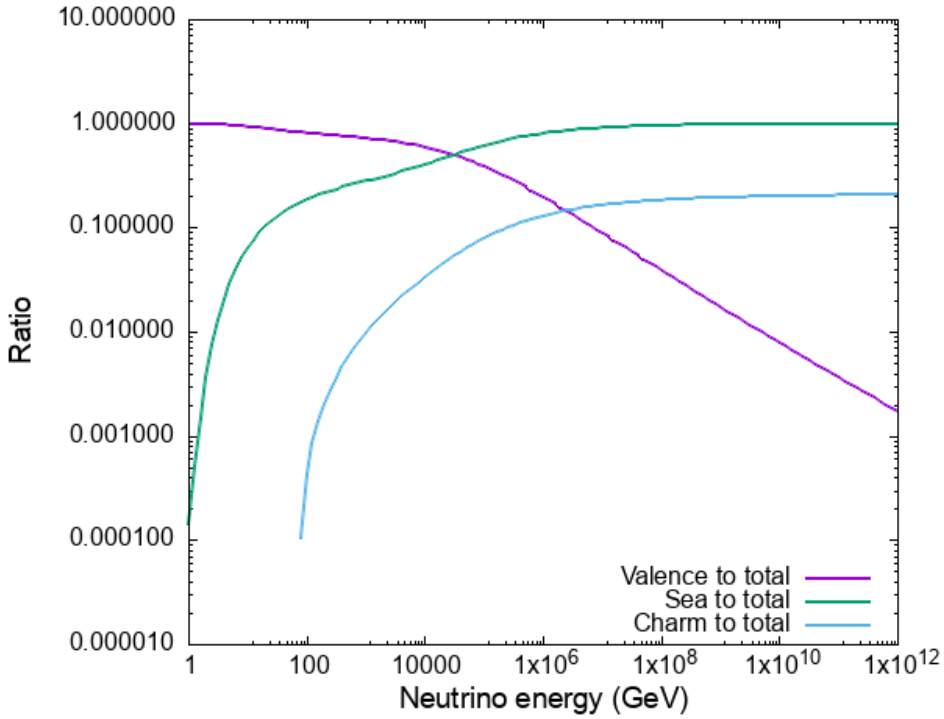


**Figure 2.6.** Ratios of different quark contributions to the total cross section in the charged current case.

As in the case of the neutral current, the ratios are functions of the neutrino energy $E_\nu$. We present the ratios graphically in Figure 2.6. Figure 2.6 demonstrates that the sea and valence quark contributions have a complementary relationship in the charged current. The valence quark contribution is the dominant contribution for low neutrino energy values, while the sea quark contribution is the dominant contribution for high neutrino energy values. In addition, the charm quark contribution increases as the neutrino energy increases. Around $10^2$ GeV, the charm contribution is at a minimum. As the neutrino energy increases, the

charm contribution increases. For neutrino energy values greater than $10^8$ GeV, the charm quark contribution does not significantly increase.

The valence and sea contribution ratios of the neutral and charged currents are similar to each other. The similarity indicates that the ratios of the valence and sea contributions do not depend on the nature of the interaction between a neutrino and a nucleon. On the other hand, for all neutrino energy values the charm quark contribution ratio is approximately equal in charged current and the neutral current and is about 20%.

# Chapter 3

# Heavy Quark Contributions

## 3.1 Cross Sections for Heavy Quarks

In the previous section, we discussed the cross section for light quarks (e.g., up, down, strange) as well as charm quarks. Although the theory of cross section of light quarks is suitable for analyzing the production of light quarks in neutrino-nucleon interactions, we need to account for the production of very heavy quarks (i.e., bottom and top quarks). For example, the cross section differential for light quarks does not include the production of bottom and top quarks [17]. We will include the heavy quarks using the calculation of [20] via the method presented in [19].

Since the bottom and top quarks are the most massive quarks, the rate of production of these quarks are much lower compared to those of lighter quarks.

The cross section again can be expressed as [15, 19, 21, 22]

$$\begin{aligned}\frac{d^2\sigma}{dx\,dy} = \frac{{G_F}^2 M E_\nu}{\pi}\left(\frac{{M_i}^2}{Q^2+{M_i}^2}\right)^2 \\ \cdot\left\{\frac{(1+(1-y)^2}{2}F_2^\nu(x,Q^2) - \frac{y^2}{2}F_L^\nu(x,Q^2) \pm y\left(1-\frac{y}{2}\right)xF_3^\nu(x,Q^2)\right\},\end{aligned} \tag{3.1}$$

where $F_i^\nu$ are appropriate structure functions. These structure functions can be calculated within the collinear factorization model as

$$F_{1,\,3} = \int dz \frac{G(z,\hat{s})}{z} f_{1,3}\left(\frac{x}{z}, Q^2\right) \tag{3.2}$$

$$F_2 = \int dz \frac{G(z,\hat{s})}{z} f_2\left(\frac{x}{z}, Q^2\right), \tag{3.3}$$

where $G$ is the gluon distribution and $a$ is defined as

$$a = 1 + \frac{(m+m')^2}{Q^2} \tag{3.4}$$

Functions $f_i$ have been calculated and defined in [20]. We incorporate these terms in the inclusive cross section for heavy quarks. Using Equation 3.1 together with the functions $f_i$ and gluon distribution obtained from [19], we obtain the cross-section in both the neutral and charged currents for heavy quarks. There are a total of three neutral current interactions ($b\bar{b}$, $t\bar{t}$, $c\bar{c}$) and two charged current interactions ($c\bar{s}$ and $b\bar{t}$). As discussed later, we shall also compute the $s\bar{s}$ contribution using this formalism, even though strange is a light quark. The presented formalism is also appropriate for lighter quark. This will serve as a comparison to the calculation with heavy quarks. To simulate these interactions, the appropriate masses must be selected. The masses of the six quark flavors are given in Table 1.1. It is worth noting that the masses of the antiquarks are the same as their quark counterparts.

When we calculate the heavy quark cross sections, we must take interactions between neutrinos and gluons into account. The main production mechanism for the heavy quarks is stemming from the boson-gluon fusion [20]. As a result, we must consider the convolution of gluons when integrating the cross section differentials.

## 3.2 Methods of Numerical Integration

To implement the numerical integration of the differential of the cross sections given in Equation 3.1, we use Monte Carlo integration method and Gaussian integration method. The Gaussian integration method was used in the code which calculated cross sections in [19]. In the Monte Carlo integration method, we select random values of $x$, $Q^2$, and $z$ in the region of integration and perform integration over bins that subdivide the region of integration. On the other hand, in the Gaussian integration method, we perform a quadrature over each single-valued integral over $x$, $Q^2$, and $z$. Monte Carlo integration is the preferred method of numerical integration, since we do not need to establish quadratures over $x$, $Q^2$, and $z$. We use a plain Monte Carlo routine provided by the GNU Scientific Library [23].

We integrate the cross section differential as

$$\sigma = \iiint dx\, dQ^2\, dz \frac{d^3\sigma}{dx\, dQ^2\, dz}. \tag{3.5}$$

In the integral, the maximum bounds of integration are

$$X_{\min} \leq x \leq 1, \tag{3.6}$$

$$Q^2_{\min} \leq Q^2 \leq K, \tag{3.7}$$

$$X_{\min} \leq z \leq 1 \tag{3.8}$$

where $K$ is defined as

$$K = \min(Q^2_{max}, s - (m + m')^2). \tag{3.9}$$

In practice the bounds of integration are different as they reflect the kinematical constraints on different variables. In the Monte Carlo integration, we cannot directly use these bounds of integration. The Monte Carlo integration method requires a rectangular region of integration.

To encompass the region required by the Monte Carlo integration method, we define a new cross section differential for the neutral current as

$$\frac{d^3\sigma^{NC,new}}{dx\, dQ^2\, dz} = \begin{cases} \frac{d^3\sigma^{NC}}{dx\, dQ^2\, dz} & X_{\min} \leq x \leq 1, Q^2_{\min} \leq Q^2 \leq K, X_{\min} \leq z \leq 1 \\ 0 & \text{otherwise} \end{cases} \tag{3.10}$$

The cross section differential is now defined in a rectangular region and can therefore be integrated using the Monte Carlo integration method. Similarly, we define a new cross section differential for the charged current as

$$\frac{d^3\sigma^{CC,new}}{dx\, dQ^2\, dz} = \begin{cases} \frac{d^3\sigma^{CC}}{dx\, dQ^2\, dz} & X_{\min} \leq x \leq 1, Q^2_{\min} \leq Q^2 \leq K, X_{\min} \leq z \leq 1 \\ 0 & \text{otherwise} \end{cases} \tag{3.11}$$

The relations between the kinematical variables $y, z, x, Q^2$ are then implemented as appropriate Heaviside functions (or cuts) inside the integrands.

## 3.3 Integrating Heavy Quark Cross Sections Using Monte Carlo Integration Method

The cross sections for the heavy quarks in the neutral current and the charged current can be numerically evaluated using the both the Gaussian and Monte Carlo methods. Using calculated cross sections, we checked that the both methods give the same results. Because the two methods give practically identical results, we present results from the Monte Carlo method in this work. Then, in both the neutral current and the charged current, we evaluate the cross section in terms of the neutrino energy $E_\nu$. Using the numerical values of $E_\nu$ and the cross section $\sigma$, we can obtain $\sigma$ vs. $E_\nu$ graphs similar to the ones presented in Chapter 2. The cross section for the neutral current and the cross section for the charged current are presented in Figure 3.1 and Figure 3.2, respectively.

In Figure 3.1, we observe that the neutral cross sections of the heavy quarks follow similar trends as the neutral cross sections of the light quarks. In all of the neutral heavy quark interactions, the cross section of the neutrino-nucleon interaction increases as the energy of the neutrino increases. For comparison, we also evaluated the cross section for the strange quark using the formula which includes masses, since it is applicable also in this case. It is worth noting that the production of strange quarks has the greatest cross section contribution, which is not surprising, since the strange quark is a light quark. As a result, it is expected that strange quarks are the most common quarks generated in neutrino-nucleon collisions. The high production of strange quarks in neutrino-nucleon collisions aligns with prior speculations about the strange quarks [10]. We clearly observe the hierarchy of cross sections according to masses: the lightest quarks are produced most abundantly. In addition, the top quark production has the least contribution to the cross section. For neutrino energy values below $10^5$ GeV, the contribution of the top quark vanishes. As a result, for insufficiently energetic neutrino-nucleon collisions, top quarks are not produced. The top quark is the most massive of the six quarks [1], so it is expected that the top quark cross section has a highest cutoff energy.

In Figure 3.2, we see that the bottom-top cross section and the charged-strange section follow similar trends as the charged cross sections of the light quarks. In both of the charged heavy quark interactions, the cross section of the neutrino-nucleon interaction increases as the energy of the neutrino increases. We observe that cross sections of bottom-top quark interactions are less than those of charm-strange interactions. As a result, bottom-top interactions occur less frequently than charm-strange interactions. Furthermore, we notice that both of the charged current interactions have cutoff energy values of $10^5$ GeV. As a result, for insufficiently high neutrino energy values, a charged current for heavy quarks does not occur.

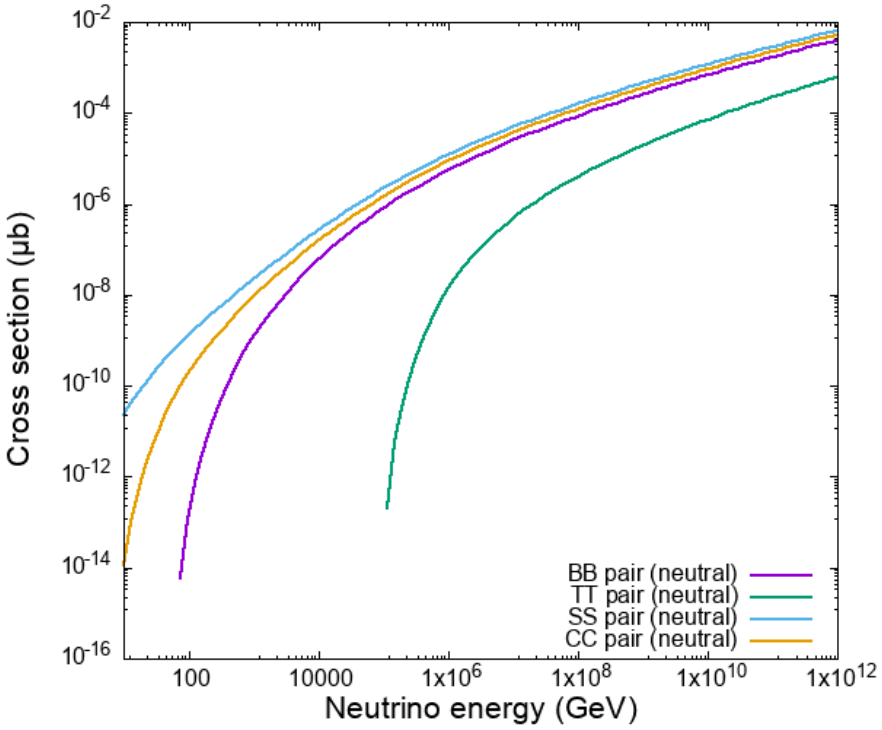


**Figure 3.1.** Cross sections with heavy quarks in neutral current case.

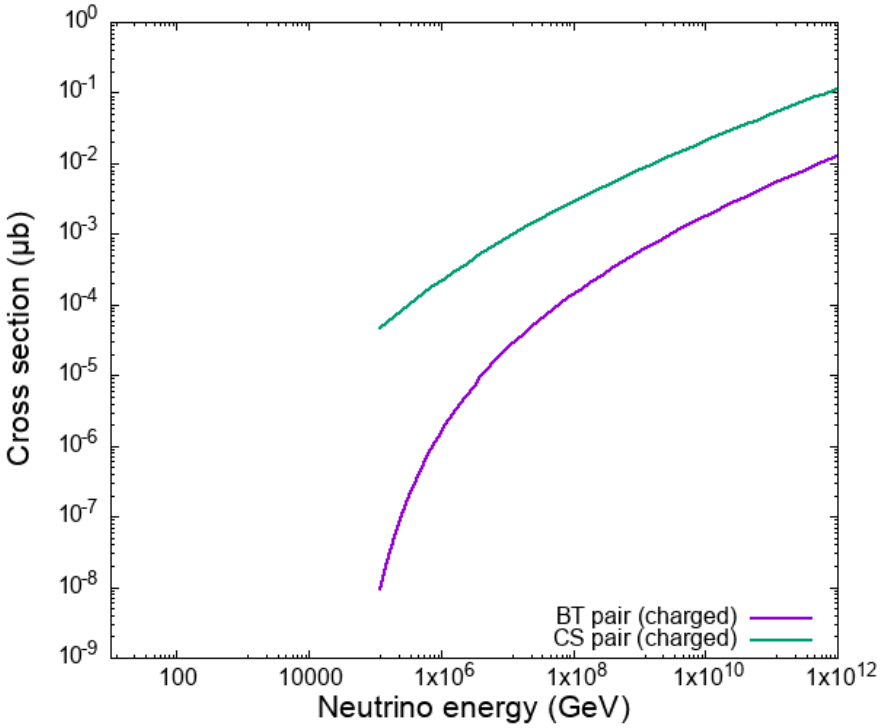


**Figure 3.2.** Cross sections with heavy quarks in charged current case.

# Chapter 4

# Inelasticity Distributions

## 4.1 Inelasticity

Inelasticity distributions for neutrino-nucleon interactions are essential for understanding neutrino-nucleon interactions in both the Standard Model and beyond [17]. For example, inelasticity of neutrino interactions is extracted and analyzed in [17], and the distribution of the average inelasticity is analyzed in [6].

In the previous chapters, we analyzed the cross section in terms of $x$, $Q^2$, and $z$. However, when we consider the inelasticity distribution, we must change the variables. In particular, we use the relationship

$$dy = \frac{dQ^2}{xs}. \tag{4.1}$$

The equation can be applied to both the neutral and charged currents. Therefore, for both the neutral current and the charged current, we can drop the dependence of the cross section on the elasticity. Using the relationship given in Equation 4.1, we can analyze the mean value of the inelasticity as it varies with energy. We define the average value of the inelasticity as

$$\langle y \rangle = \frac{\int dy\, y\, \frac{d\sigma}{dy}}{\int dy\, \frac{d\sigma}{dy}} \tag{4.2}$$

Notice that

$$\frac{d\sigma}{dy} = \int dx\, dz\, \frac{d\sigma}{dx\, dy\, dz} \equiv f(y), \tag{4.3}$$

where $f(y)$ is some function that satisfies the definition of $\frac{d\sigma}{dy}$. Furthermore, we define a function g such that

$$g(E_\nu) = \frac{\int dy\, y\, \frac{d\sigma}{dy}}{\int dy\, \frac{d\sigma}{dy}}. \tag{4.4}$$

Thus, combining Equations 4.3 and 4.4, we get

$$g(E_\nu) = \int \frac{dy\, y\, f(y)}{f(y)}, \tag{4.5}$$

which can be used to calculate the distribution of the energy. As a result, we can compute the distribution $h^{NC}$ of the neutral cross section in terms of the inelasticity as follows.

$$h^{NC}(E_\nu) = \int dx\, dy\, y\, \frac{d^2\sigma^{NC}}{dx\, dy} \tag{4.6}$$

Similarly, for the charged current, the distribution $h^{NC}$ is

$$h^{CC}(E_\nu) = \int dx\, dy\, y\, \frac{d^2\sigma^{CC}}{dx\, dy}. \tag{4.7}$$

## 4.2 Numerical Results for Inelasticity

Using the equations given in Section 4.1, we obtain numerical results for $d\sigma/dy$ distributions and $\langle y \rangle$ distributions. For our purposes, we use a neutrino energy value of $E_\nu = 10^{12}$ GeV. Graphs of the numerical results are presented in Figures 4.1 to 4.8.

According to Figures 4.1 to 4.4, the value of $d\sigma/dy$ in general decreases as the inelasticity $y$ increases. In other words, the more inelastic a neutrino-nucleon interaction is, the less the value of $d\sigma/dy$ is. The fact that the average value is zero below $10^2$ GeV (for charm and strange) and $10^6$ GeV (for bottom-top case) is due to the cutoff in the calculation to ensure that the cross section is calculated above the kinematic threshold.

In Figures 4.5 to 4.8, the average value of the inelasticity is shown for $b\bar{b}, bt, c\bar{c}, cs$ cases as a function of the energy of the neutrino. We observe that the average value of inelasticity is a decreasing function of the energy. For the case of the neutral current, $c\bar{c}$ and $b\bar{b}$ production, the average inelasticity saturates at high energies to about 0.4. For the case of the charged current, the average inelasticity levels at high energies to a value ranging from 0.2 to 0.3. According to the results presented in [6], the average value of the inelasticity levels to about 0.2 for both the neutral current and the charged current. Similarly, according to the results presented in [17], the inelasticity levels to between 0.2 and 0.3 for the charged current.

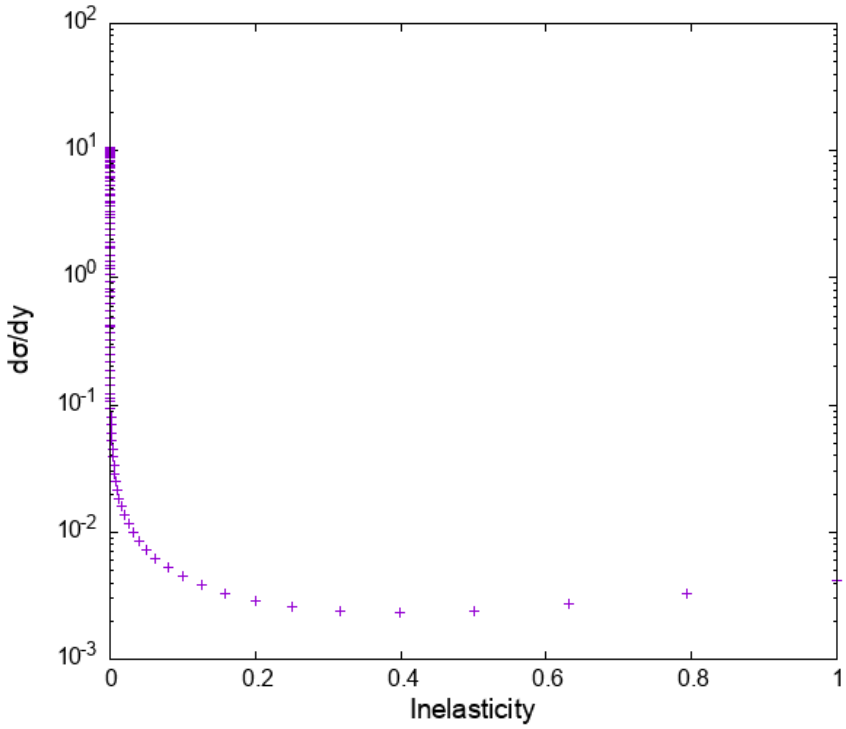


**Figure 4.1.** $d\sigma/dy$ distribution for $b\bar{b}$ case in the neutral current.

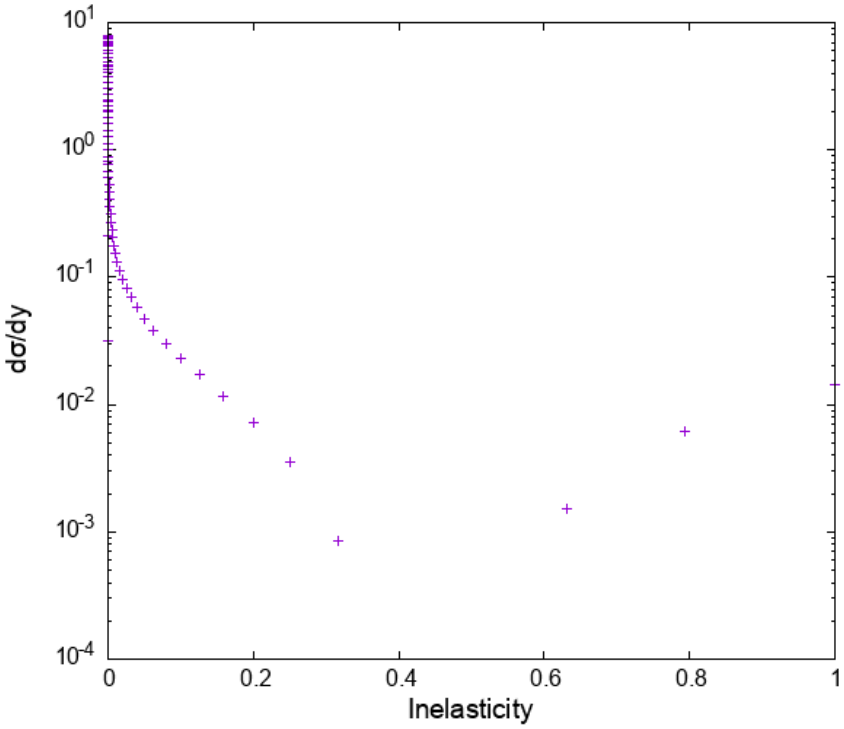


**Figure 4.2.** $d\sigma/dy$ distribution for $bt$ case in the charged current.

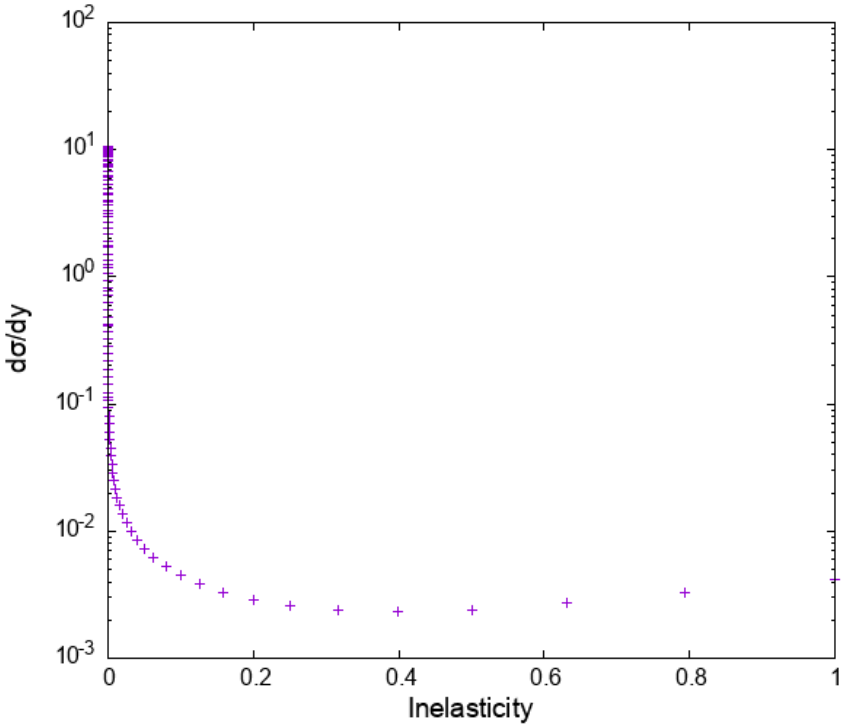


**Figure 4.3.** $d\sigma/dy$ distribution for $c\bar{c}$ in the neutral current case.

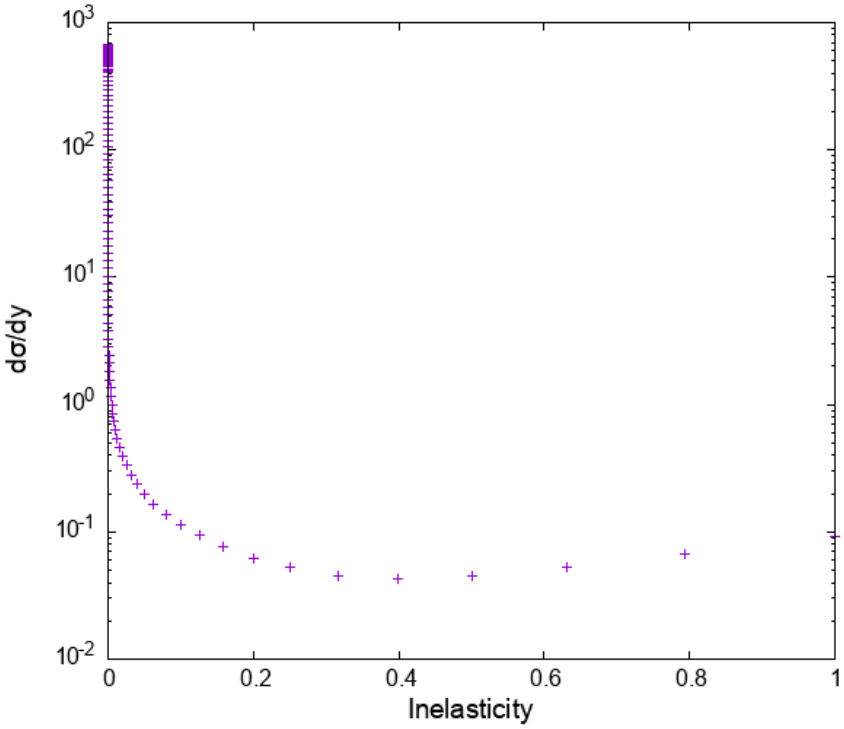


**Figure 4.4.** $d\sigma/dy$ distribution for $sc$ in the charged current case.

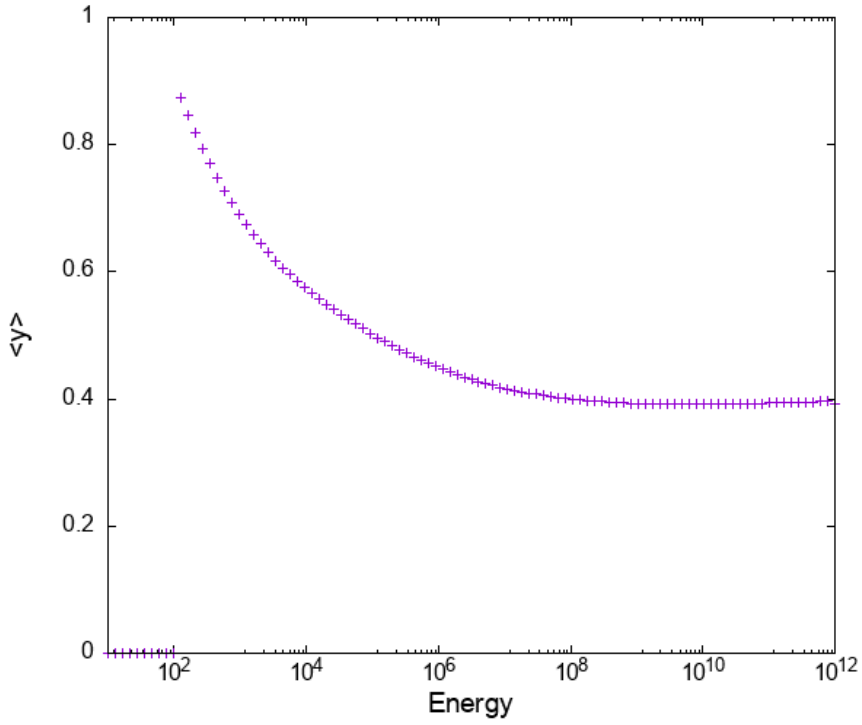


**Figure 4.5.** Average inelasticity $\langle y \rangle$ as a function of the neutrino energy for $b\bar{b}$ in the neutral current case.

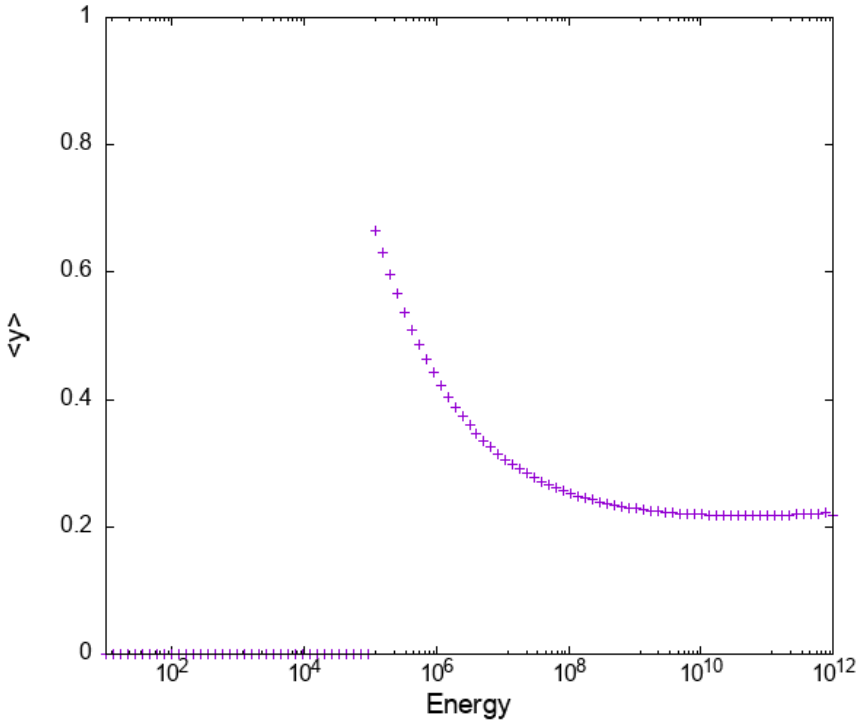


**Figure 4.6.** Average inelasticity $\langle y \rangle$ as a function of the neutrino energy for $bt$ in the charged current case.

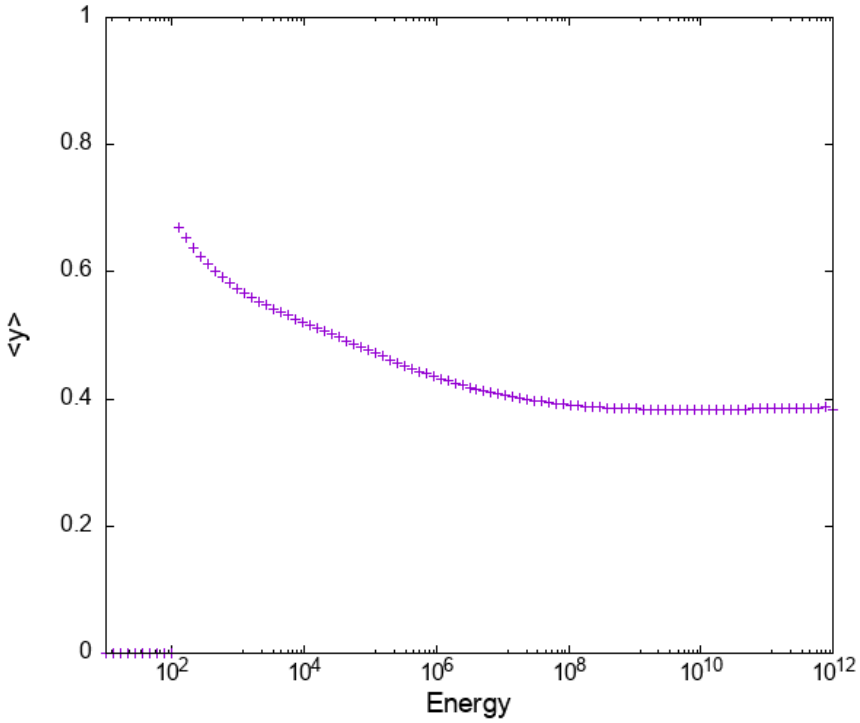


**Figure 4.7.** Average inelasticity $\langle y \rangle$ as a function of the neutrino energy for $c\bar{c}$ in the neutral current case.

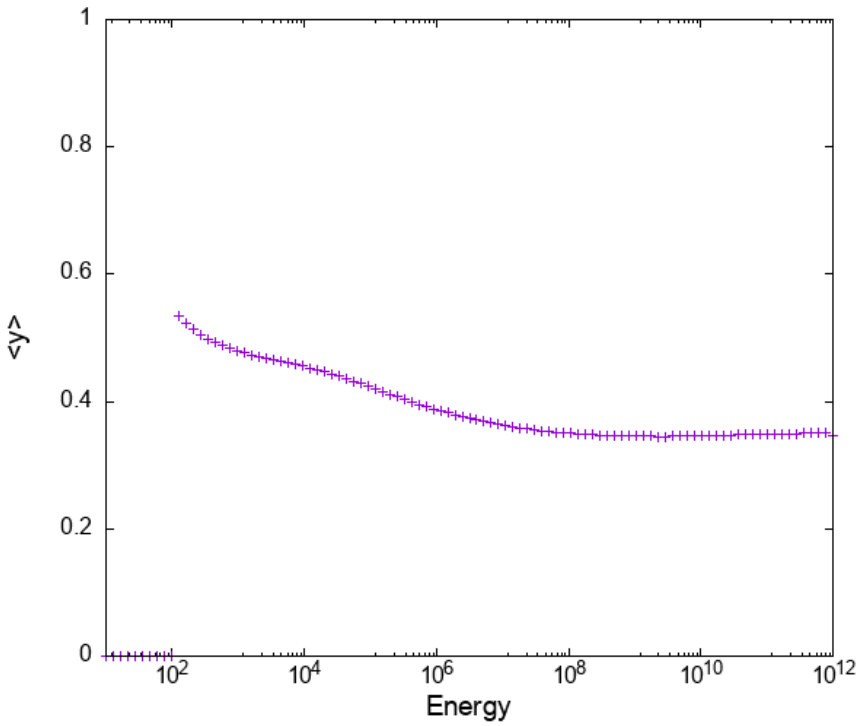


**Figure 4.8.** Average inelasticity $\langle y \rangle$ as a function of the neutrino energy for *sc* in the charged current case.

# Chapter 5

# Conclusions

Using numerical simulations of the cross section of neutrino-nucleon interactions, we study the dependence of the cross section of extremely energetic neutrino-nucleon interactions as a function of the energy of the incoming neutrino. By expressing the cross section in terms of the parameters of the Bjorken scaling $x$, the transfer of the four-momentum $Q^2$, and the fractional energy loss $z$, we numerically obtain a power law of the cross section of the neutrino-nucleon in terms of the neutrino energy. Furthermore, using numerical calculations of the cross section values, we obtain ratios of the charm, valence, and sea contributions.

We also use cross section to analyze the heavy quark production of particles. As expected, the cross sections for the neutral current interactions (i.e., top-bottom, bottom-bottom, charm-charm, charm-strange) increase as the energy of the neutrino increases. The increase in the cross sections for the heavy quarks is analogous to the increase in those for the light quarks.

Finally, we use our calculated cross section values to obtain distributions related to the inelasticity. According to our analysis of the relationship between the cross section and the inelasticity, the differential cross section with in the inelasticity decreases as the inelasticity $y$ approaches the maximum value of 1. We also evaluate the average values of the inelasticity as a function of the energy of the neutrino for different heavy quarks in the neutral and charged current cases.

# Bibliography


[1] David Griffiths. *Introduction to Elementary Particles*. Wiley-VCH, 2nd edition, 2008.

[2] Anna Stasto. Physics of ultrahigh energy neutrinos. *Int. J. Mod. Phys. A19:317-340*, 2004.

[3] John N. Bahcall et al. Progress and prospects in neutrino astrophysics. *Nature volume 375, 29–34*, 1995.

[4] Francis Halzen and Dan Hooper. High-energy neutrino astronomy: The cosmic ray connection. *Rept. Prog. Phys. 65:1025-1078*, 2002.

[5] IceCube. `https://icecube.wisc.edu/science/icecube/`.

[6] Raj Gandhi et. al. Ultrahigh-energy neutrino interactions. *Astropart. Phys. 5:81-110*, 1996.

[7] Karl Mannheim. Frontiers in high-energy astroparticle physics. *Rev.Mod.Astron.12:101-120*, 1999.

[8] K. Abe et al. Search for neutrinos in super-kamiokande associated with the gw170817 neutron-star merger. *The Astrophysical Journal Letters, Volume 857, Number 1*, 2018.

[9] Thomas K. Gaisser, Francis Halzen, and Todor Stanev. Particle astrophysics with high energy neutrinos. *Phys.Rept.258:173-236*, 1995.

[10] Atri Bhattacharya et al. Perturbative charm production and the prompt atmospheric neutrino flux in light of rhic and lhc. *Journal of High Energy Physics*, 2015.

[11] V.A. Li et al. Studies of mcp-pmts in the minitimecube neutrino detector. *AIP Advances 8, 095003*, 2018.

[12] J. Ahrens et al. Recent results from the amanda experiment. *38th Rencontres de Moriond on Electroweak Interactions and Unified Theories*, 2003.

[13] Paolo Desiati. Neutrino astronomy at the south pole: Status of the amanda experiment. *Frascati Phys.Ser. 30 (2003) 45-62*, 2003.

[14] Sheldon L. Glashow. Resonant scattering of antineutrinos. *Phys. Rev. 118, 316*, 1960.

[15] Francis Halzen and Alan D. Martin. *Quarks & Leptons: An Introductory Course in Modern Particle Physics*. John Wiley & Sons, 1984.

[16] Joseph A. Formaggio. From ev to eev: Neutrino cross-sections across energy scales. *Rev. Mod. Phys. 84, 1307*, 2012.

[17] M.G. Aartsen et al. (IceCube Collaboration). Measurements using the inelasticity distribution of multi-tev neutrino interactions in icecube. *Phys. Rev. D 99, 032004*, 2019.

[18] H. Abramowicz et al. Combination of measurements of inclusive deep inelastic $e^{\pm}p$ scattering cross sections and QCD analysis of HERA data. *Eur. Phys. J. C*, 75(12):580, 2015.

[19] J. Kwiecinski, A.D. Martin, and A.M. Stasto. Penetration of the earth by ultrahigh energy neutrinos predicted by low $x$ qcd. *Phys. Rev. D 59, 093002*, 1999.

[20] M. Glück, R.M Godbole, and E. Reya. Heavy flavor production at high energy ep colliders. *Particles and Fields 38, 441-447*, 1988.

[21] R. G. Roberts. *The Structure of the Proton: Deep Inelastic Scattering*. Cambridge University Press, 1990.

[22] R. K. Ellis, W. J. Stirling, and B. R. Webber. *QCD and Collider Physics*. Cambridge University Press, 1996.

[23] GNU. `https://www.gnu.org/software/gsl/doc/html/montecarlo.html`.

# Academic Vita

**Henry Li**

## Education

B.S. in Physics (with Honors), Pennsylvania State University (2024)

B.S. in Mathematics, Pennsylvania State University (2024)

## Research Work Experience

- Developed mathematical models and conducted computer simulations of subatomic particles, 2023 Spring and Fall Semesters at Penn State University
  - Constructed mathematical models for the cross sections of neutrino-nucleon interactions
  - Analyzed the relationship between charm, valence, and sea quark contributions
  - Obtained a power law for the cross section and neutrino energy
  - Analyzed cross sections associated with heavy quarks
  - Used simulations to investigate the distribution of the inelasticity
- Developed mathematical models and numerical methods to analyze quantum cosmology, 2023 Summer Penn State University Physics REU
  - Developed a Hamiltonian for an expanding universe
  - Constructed a quantum cosmological model using local clocks
  - Incorporated curvature of spacetime into the quantum cosmological model
  - Mathematically demonstrated that the volume of an expanding universe oscillates
  - Investigated the role of the phase of oscillations on the volume of the universe
- Developed computer simulations of gravitational waves, 2022 Summer Internship at Penn State University
  - Developed approximants for calculating the strain and amplitude of gravitational waves
  - Developed computer simulations to demonstrate the effect that masses of binary black holes pairs had on resulting gravitational waves

## Awards and Honors

- Schreyer Honors College at Penn State University
- Sigma Pi Sigma, The Physics Honor Society

- John and Elizabeth Holmes Teas Scholarship at Penn State University (2023-2024)
- Evan Pugh Scholar Award at Penn State University (2023)
- Elsbach Honors Scholarship in Physics at Penn State University (2022-2023)
- President Sparks Award at Penn State University (2022)
- President's Freshman Award at Penn State University (2021)
- Homer Braddock Scholarship at Penn State University (2021-2024)
- Penn State Lehigh Valley Chancellor's Promising Student Award (2020-2021)